Published February 1, 1997

Electrodiffusion, Barrier, and Gating Analysis of DIDS-insensitive Chloride Conductance in Human Red Blood Cells Treated with Valinomycin or Gramicidin

JEFFREY C. FREEDMAN and TERRI S. NOVAK

From the Department of Physiology, State University of New York Health Science Center, Syracuse, New York 13210

ABSTRACT Current-voltage curves for DIDS-insensitive Cl^- conductance have been determined in human red blood cells from five donors. Currents were estimated from the rate of cell shrinkage using flow cytometry and differential laser light scattering. Membrane potentials were estimated from the extracellular pH of unbuffered suspensions using the proton ionophore FCCP. The width of the Gaussian distribution of cell volumes remained invariant during cell shrinkage, indicating a homogeneous Cl^- conductance among the cells. After pretreatment for 30 min with DIDS, net effluxes of K^+ and Cl^- were induced by valinomycin and were measured in the continued presence of DIDS; inhibition was maximal at ~65% above 1 μM DIDS at both 25°C and 37°C. The nonlinear current-voltage curves for DIDS-insensitive net Cl^- effluxes, induced by valinomycin or gramicidin at varied $[K^+]_o$, were compared with predictions based on (*1*) the theory of electrodiffusion, (*2*) a single barrier model, (*3*) single occupancy, multiple barrier models, and (*4*) a voltage-gated mechanism. Electrodiffusion precisely describes the relationship between the measured transmembrane voltage and $[K^+]_o$. Under our experimental conditions (pH 7.5, 23°C, 1–3 μM valinomycin or 60 ng/ml gramicidin, 1.2% hematocrit), the constant field permeability ratio P_K/P_{Cl} is 74 ± 9 with 10 μM DIDS, corresponding to 73% inhibition of P_{Cl}. Fitting the constant field current-voltage equation to the measured Cl^- currents yields $P_{Cl} = 0.13\ h^{-1}$ with DIDS, compared to $0.49\ h^{-1}$ without DIDS, in good agreement with most previous studies. The inward rectifying DIDS-insensitive Cl^- current, however, is inconsistent with electrodiffusion and with certain single-occupancy multiple barrier models. The data are well described either by a single barrier located near the center of the transmembrane electric field, or, alternatively, by a voltage-gated channel mechanism according to which the maximal conductance is 0.055 ± 0.005 S/g Hb, half the channels are open at −27 ± 2 mV, and the equivalent gating charge is −1.2 ± 0.3.

KEY WORDS: erythrocyte membrane • ion transport • chloride channels • band 3 protein • membrane potentials

INTRODUCTION

The transport of carbon dioxide from the tissues to the lungs is facilitated by the formation of bicarbonate by red blood cells in a cyclic reaction scheme known as the Jacobs-Stewart cycle (Jacobs and Stewart, 1942; for review, see Klocke, 1988). The hydration of carbon dioxide to carbonic acid, catalyzed by red cell carbonic anhydrase, and then its dissociation into bicarbonate, is followed by rapid electroneutral exchange of bicarbonate for Cl^- across the red cell membrane. These reactions increase the carbon dioxide carrying capacity of the blood, while minimizing acidification of venous blood. Red cell Cl^-/HCO_3^- exchange, known as the "Hamburger shift" or "chloride shift", is mediated by the membrane domain of capnophorin, a protein also denoted as anion exchanger AE1. This integral glycoprotein (mol wt 101,700) comprises 25% of the mass of membrane protein in red blood cells and is the predominant protein located in band 3 of SDS polyacrylamide gels (for reviews see Knauf, 1979; Passow, 1986; Jennings, 1989, 1992; Reithmeier, 1993).

In addition to electroneutral anion exchange, capnophorin is also thought to mediate a small conductive net anion flux, which could be important as the rate limiting step for electrolyte and water movements during patho-physiological dehydration of the red cell (Freedman et al., 1988). Previous studies of conductive anion fluxes mediated by red cells treated with the irreversible covalent inhibitor DIDS revealed DIDS-sensitive and DIDS-insensitive components of the net Cl^- fluxes (Knauf et al., 1977; Kaplan et al., 1983). DIDS is the most potent of a series of stilbene derivatives originally found by Cabantchik and Rothstein (1972) specifically to inhibit red cell anion transport. In our studies of anion conductance with human red blood cells, we found that the DIDS-insensitive component of net anion efflux increases with increasing extents of mem-

Address correspondence to J.C. Freedman, Department of Physiology, SUNY Health Science Center, 766 Irving Avenue, Syracuse, NY 13210. Fax: 315-464-7712; E-mail: FREEDMAJ@VAX.CS.HSCSYR.EDU

Published February 1, 1997

brane hyperpolarization (Freedman and Novak, 1987; Freedman et al., 1988, 1994).

Models for the mechanism of conductive ion transport can be tested and are constrained by the characteristic current-voltage and conductance-voltage relationships (e.g., Hodgkin and Huxley, 1952; Läuger, 1973). In the equivalent circuit shown in Fig. 1, the K^+, Na^+, and Cl^- concentration gradients across the red cell membrane are represented as batteries (E_K, E_{Na}, and E_{Cl}) in parallel with the membrane capacitance C_m. Each battery is in series with its respective ionic conductance (g_K, g_{Na}, and g_{Cl}). The electrical potential inside the cell is E_m, while that outside is at ground. Because it has not proven possible to use microelectrodes to drive currents or to clamp the voltage across the human red cell membrane (Lassen, 1972), ionophores have been used instead to increase the permeability to cations, thus permitting ionic currents to flow under the influence of diffusion potentials, which can then be measured indirectly. Treatment of red cells with valinomycin, or with gramicidin in sodium-free medium, increases g_K above the normally low value of g_{Cl} and allows the flow of the ionic currents, i_K and i_{Cl} (Fig. 1, *arrows*); the net efflux of K^+ and Cl^- discharges the potassium battery while charging the chloride battery. The K^+ and Cl^- currents are opposite in sign and approximately equal in magnitude; a small disparity (within 10%) at hyperpolarizing voltages is accounted for by proton fluxes (Freedman et al., 1994). Whereas the total net current across the membrane is zero in the absence of an external circuit, the individual ionic currents induced by the addition of ionophores can be measured directly, or, as in the present study, inferred from the rate of cell shrinkage. Fluorescent potentiometric indicators that monitor the voltages continuously show that the voltage is indeed clamped at a steady value after the addition of valinomycin or gramicidin; steady levels of dye fluorescence are seen with the oxacarbocyanine dye, diO-C_6(3) (Hoffman and Laris, 1974), or with the thiadicarbocyanine, diS-C_3(5), or indodicarbocyanine, diI-C_3(5), dyes (Freedman and Hoffman, 1979; Freedman and Novak, 1989). In the present study, the change in voltage has been estimated from the change in the extracellular pH of unbuffered DIDS-treated red cell suspensions (Macey et al., 1978) using the proton ionophore FCCP; we previously used this method to calibrate fluorescent potentiometric indicators (Freedman and Novak, 1983, 1989; Bifano et al., 1984). In this report, which has been briefly summarized (Freedman and Novak, 1996), we show that the inward rectifying current-voltage curve describing DIDS-insensitive Cl^- conductance is inconsistent with an electrodiffusion mechanism and with certain single-occupancy multiple barrier models, but instead is consistent either with a single barrier located near the center of the transmembrane electric field, or with a voltage-gated mechanism with an equivalent gating charge of -1.2 ± 0.3 under our experimental conditions.

MATERIALS AND METHODS

Blood from healthy human donors was drawn by venipuncture into heparinized tubes and immediately centrifuged at 13,800 *g* for 3 min at 4°C. The plasma and buffy coat were aspirated and discarded, and the packed cells were then washed three times by centrifugation, each time resuspending in about 5 vol of chilled medium containing 1 mM KCl and 149 mM NaCl for experiments with valinomycin, or 1 mM KCl and 149 mM choline chloride for experiments with gramicidin. The cells were then adjusted to 50% hematocrit (HCT) in the cold wash solution and kept on ice for use on the same day.

To determine cell potassium, $[K^+]_c$, the cells were diluted with the washing medium to 1.2% hematocrit, and were packed by centrifugation in 0.4 ml microcentrifuge tubes attached to syringe tubes as previously described (Freedman and Hoffman, 1979*a*; Freedman et al., 1994). Triplicate samples of packed cells with weight (w) (40–80 mg) were hemolyzed in 10 ml deionized water. Portions of the hemolysates were then diluted in half with 30 mM $LiNO_3$, followed by flame photometric analysis for the concentration of potassium in the hemolysate, $[K^+]_h$. $[K^+]_c$ was calculated from $[K^+]_c = [K^+]_h \cdot 2 \cdot 10/fw$, where f (g H_2O/g packed cells) is the packed cell water determined gravimetrically, in triplicate, as previously described (Freedman et al., 1994). The cellular potassium concentration, $[K^+]_c'$, corrected for trapped medium, ϵ, (0.026 ml/g packed cells, as determined previously with [^{14}C]inulin) is given by $[K^+]_c' = (f[K^+]_c - \epsilon[K^+]_o)/(f - \epsilon)$. The corrected cell water content, f' (g cell water/g cells) is obtained from $f' = (f - \epsilon)/(1 - \epsilon)$. Other portions of the same hemolysates were diluted with Drabkin's reagent, and were analyzed spectrophotometrically for hemoglobin, Hb (g/ml packed

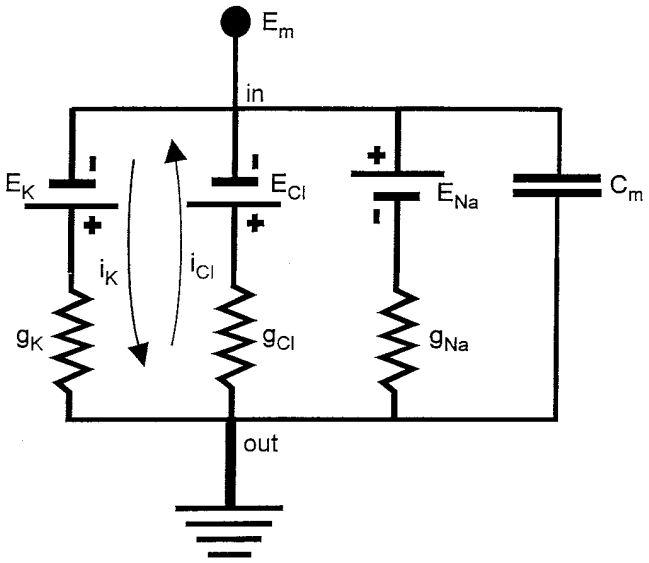

FIGURE 1. Equivalent electrical circuit for human red blood cells treated with valinomycin or gramicidin. Arrows indicate the direction of positive current flow when the potassium conductance, g_K, is increased by the addition of ionophores.

Published February 1, 1997

cell water), using cyanmethemoglobin standards; the corrected hemoglobin concentrations, Hb′ (g/ml cell water) are obtained from $Hb' = fHb/(f - \epsilon)$. The initial membrane potential, E_m, was estimated from the chloride equilibrium potential, $E_{Cl} = 58.7 \log r_{Cl}$, where the Donnan ratio, r_{Cl}, was determined in triplicate after equilibration of 1.2 percent hematocrit suspensions for 15 min with ^{36}Cl at pH 7.5 and 23°C, as previously described (Freedman et al., 1994). The Donnan ratio, r', corrected for trapped medium is obtained from $r' = (fr - \epsilon)/(f - \epsilon)$. These measurements permitted calculation of initial values of the membrane potential, $E_m = (RT/\mathcal{F})\ln r'_{Cl}$, and of the equilibrium potentials, E_K and E_{Cl}.

Current-voltage curves for DIDS-insensitive net effluxes of Cl^- and K^+ from human red blood cells treated with valinomycin or gramicidin at varied concentrations of extracellular K^+, or $[K^+]_o$, were determined as previously described (Freedman et al., 1994). The cells were diluted to 1.2% hematocrit and were pretreated with 10 μM DIDS for 30 min at 23°C. The net effluxes of K^+ and Cl^- were estimated at 23°C in the continued presence of DIDS in duplicate flasks from the rate of cell shrinkage, as measured by flow cytometry and differential laser light scattering in the Technicon H-1 Hematology Analyzer (Technicon Instruments Corporation, Tarrytown, NY). For each sample the mean cell volume, MCV, and the relative distribution width, RDW, or coefficient of variation of the Gaussian distribution of cell volumes in the cell suspension, was noted. For the experiments in Fig. 3, net effluxes of K^+ and Cl^- were determined directly by the cold-quench method, which involves stopping the efflux at desired times by inserting a cold-finger condenser into a sample of the cell suspension, separating the cells from the medium by centrifugation, and then measuring the cellular contents of K^+ by flame photometry, and of Cl^- with a chloridometer (Freedman et al., 1994). Fluxes estimated from cell volume changes are more convenient and have better time resolution, and were previously found to agree with those determined directly by the cold-quench method.

For the five current-voltage experiments shown in Fig. 5, net effluxes of chloride induced by valinomycin or gramicidin were estimated from the rate of decrease of the mean cell volume. Changes in the membrane potential were estimated in parallel in unbuffered DIDS-treated suspensions from the change in the external pH, or pH_o, from an initial pH_o of 7.5 at 23°C before DIDS, to the final steady value attained after adding 1 μM of the proton ionophore FCCP, also as described previously (Freedman et al., 1994). Controls showed that, after the initial K^+/H^+ exchange, 1 μM FCCP had no effect on the rate of cell shrinkage induced by 3 μM valinomycin in suspensions treated at 23°C with 10 μM DIDS between 1 and 150 mM $[K^+]_o$. In three other control experiments, doubling the concentration of FCCP from 1 μM to 2 μM increased the extent of hyperpolarization induced by 1 μM valinomycin at 1 mM $[K^+]_o$ by 7 ± 3 mV. The effect of FCCP in increasing the extent of hyperpolarization without significantly affecting the net efflux is consistent with a stimulation of P_K, as described by Bennekou (1984, 1988) for the related protonophore CCCP.

A curve-fitting program (Sigmaplot 4.1, Jandel Scientific, Corte Madera, CA) that uses the Marquardt-Levenberg algorithm to minimize the weighted variance of a nonlinear least squares regression on the data was used to obtain the best-fit estimates of model parameters.

RESULTS

Homogeneity of Chloride Efflux in the Cell Population

For human red blood cell suspensions treated with 10 μM DIDS at 1 mM $[K^+]_o$, the decrease in mean cell volume, MCV, relative to the initial mean cell volume, MCV^o, is linear for up to 15 min after addition of 1 μM valinomycin (Fig. 2 *A*) or 60 ng/ml gramicidin (Fig. 2 *B*). The initial mean cell volume, MCV^o, averaged 93.2 fl for the two experiments with valinomycin shown in Fig. 2 *A*, and 90.0 fl for the two experiments with gramicidin shown in Fig. 2 *B*. The linearity of the time course of the decrease of cell volume in the presence of DIDS is consistent with that previously seen in the presence or absence of DIDS (Fig. 4 in Freedman et al., 1994), and is shown here along with the relative distribution width (RDW)[1] at each time point. The results show that RDW remains relatively constant, changing by <1% in 15 min (Fig. 2, *C* and *D*). For all of the time points in two experiments with valinomycin, RDW was 13.2 ± 0.6 (SD, $n = 12$) (Fig. 2 *C*, *square*), and in two experiments with gramicidin RDW was 14.4 ± 0.3 (SD, $n = 12$) (Fig. 2 *D*, *square*). In the absence of DIDS, RDW also remained constant after addition of valinomycin or gramicidin at 1 mM $[K^+]_o$: in one experiment with six identical suspensions (Fig. 4 *A* of Freedman et al., 1994) RDW was 13.4 ± 0.3 (SD, $n = 6$) initially, and was 13.7 ± 0.3 (SD, $n = 6$) 16 min after addition of 3 μM valinomycin; in a similar experiment (Fig. 4 *B* of Freedman et al., 1994) RDW was 14.2 ± 0.3 (SD, $n = 6$) initially, and was 14.2 ± 0.5 (SD, $n = 6$) 10 min after addition of 60 ng/ml gramicidin. The invariance of the width of the Gaussian distributions of cell volume in red cell suspensions during cell shrinkage induced by valinomycin or gramicidin in the presence or absence of DIDS implies that the rate limiting permeability to Cl^- is uniform among the cells in the population. If some of the cells had a higher permeability to Cl^- than other cells, and consequently shrunk faster, then the Gaussian distribution of cell volumes would have broadened, and the value of RDW would have increased after the addition of ionophores, in contrast to the invariance of RDW that was observed. A similar conclusion concerning the homogeneity of P_{Cl} in the cell population was reached recently by Raftos et al. (1996), who estimated the distribution of Cl^- permeabilities indirectly by measuring the slope of the osmotic fragility curve of red cells taken at different times after the addition of valinomycin.

Effect of Varied [DIDS] on Net K^+ and Cl^- Efflux at 23°C and 37°C

With the membrane potential measured by using the proton ionophore CCCP, Bennekou and Stampe (1988) reported at least 95% inhibition of Cl^- conductance by DIDS at 37°C. They attributed the disparity between this rather complete inhibition, and the 62–72%

[1] *Abbreviation used in this paper:* RDW, relative distribution width.

Published February 1, 1997

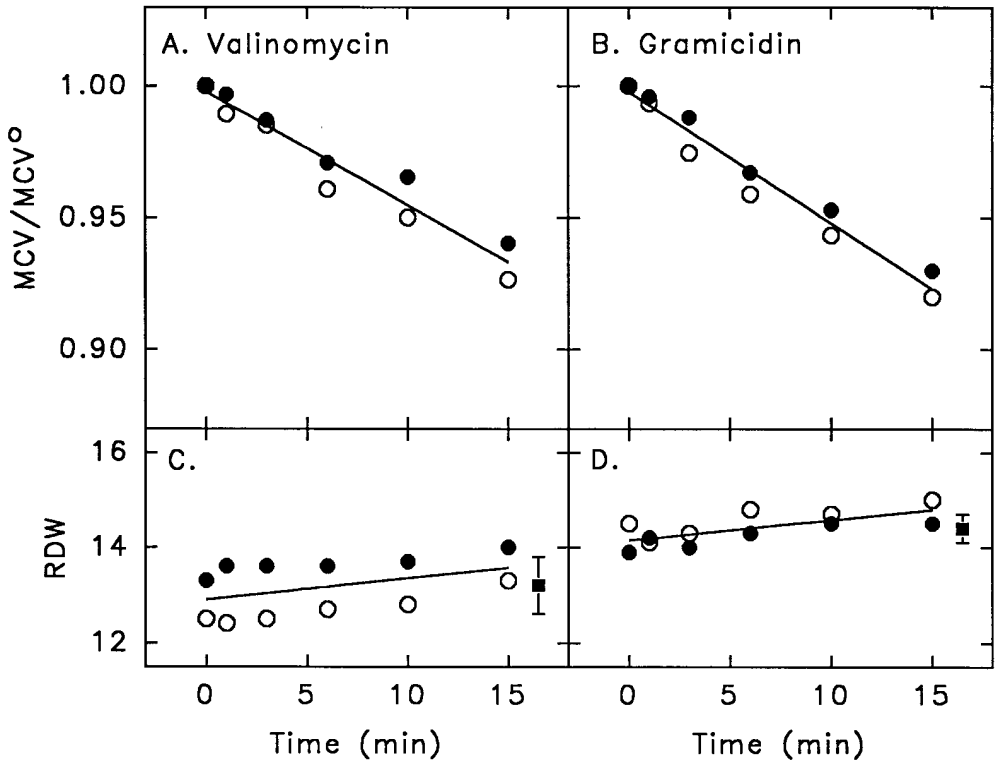

FIGURE 2. (*A* and *B*) Decrease of mean cell volume, MCV, relative to initial mean cell volume, MCV^o, induced by addition of 1 μM valinomycin (*A*) or 60 ng/ml gramicidin (*B*). Washed human red blood cells at 1.2 percent hematocrit were pretreated with 10 μM DIDS for 30 min at 23°C in medium containing 1 mM KCl and 149 mM NaCl (for valinomycin), or 1 mM KCl and 149 mM choline chloride (for gramicidin); after addition of ionophore, the mean cell volumes were measured at the times indicated (see MATERIALS AND METHODS). Points represent average values of samples from duplicate flasks; the filled and empty symbols refer to two experiments, and the solid lines are linear regressions. (*C* and *D*) Time course of the relative distribution width (RDW) or coefficient of variation of the Gaussian distributions of cell volume, determined for each sample in the experiments in *A* and *B* after addition of valinomycin (*C*) or gramicidin (*D*). Filled squares represent mean ± SD ($n = 12$) for all of the points in the respective time course.

partial inhibition of P_{Cl} repeatedly seen by others (Knauf et al., 1977, 1983; Kaplan et al., 1983), to the use in prior studies of the constant field theory, and they questioned the existence of a DIDS-insensitive component of anion fluxes across human red blood cell membranes. For cells pretreated with varied [DIDS], we previously reported that the degree of inhibition by DIDS of the efflux of K^+ induced by 1 μM valinomycin at 1 mM $[K^+]_o$ reaches a maximum of 65% at 23°C (Freedman and Novak, 1987; Fig. 7 in Freedman et al., 1994), in agreement with the partial inhibition reported by others (Knauf et al., 1977, 1983; Kaplan et al., 1983). The experiments whose results are shown in Figs. 3–4 test whether or not the differing experimental conditions might influence the existence of the DIDS-insensitive fluxes. The results in Fig. 3 show the effluxes of K^+ (*circles*) and of Cl^- (*squares*) induced by 3 μM valinomycin at varied [DIDS] at both 23°C, the temperature we used previously (Freedman et al., 1988, 1994), and at 37°C, the temperature used by Bennekou and Stampe (1988). The results show that the inhibition of the fluxes is maximal above about 1 μM DIDS, but remains partial at around 65% at both temperatures. The percent inhibition of the fluxes themselves at a particular $[K^+]_o$ is less than the inhibition of Cl^- conductance because the membrane potential hyperpolarizes, and the driving force increases, with increasing [DIDS]. Thus, an inhibited flux divided by an increased driving force yields a conductance which has a greater percent inhibition than that of the flux itself. The partial inhibition persists, however, when either P_{Cl} or the Cl^- conductance are estimated from measured net effluxes of Cl^- and from measured membrane potentials (Freedman and Novak, 1987; Freedman et al., 1994; and Fig. 5 *A* as discussed below).

Effect of Varied Duration of Pretreatment with DIDS

In the experiments of Bennekou and Stampe (1988), the fluxes were reportedly determined during the first 90 s after adding cells to medium containing DIDS at 37°C, with the flux initiated by addition of valinomycin. Longer times were used to determine the slower fluxes (Stampe, P., personal communication). Conceivably, the cells might have had a mixture of reversibly and irreversibly bound DIDS, depending on the time of exposure to DIDS. DIDS is known to react with capnophorin in at least two steps: a reversible binding leading to complex I, followed by a slower irreversible covalent reaction leading to complex II as follows:

$$\underset{\text{band 3}}{\text{DIDS} + \text{band 3}} \underset{\text{I}}{\leftrightarrow \text{DIDS} \quad \text{band 3}} \rightarrow \underset{\text{II}}{\text{DIDS} \cdot \text{band 3}}.$$

Published February 1, 1997

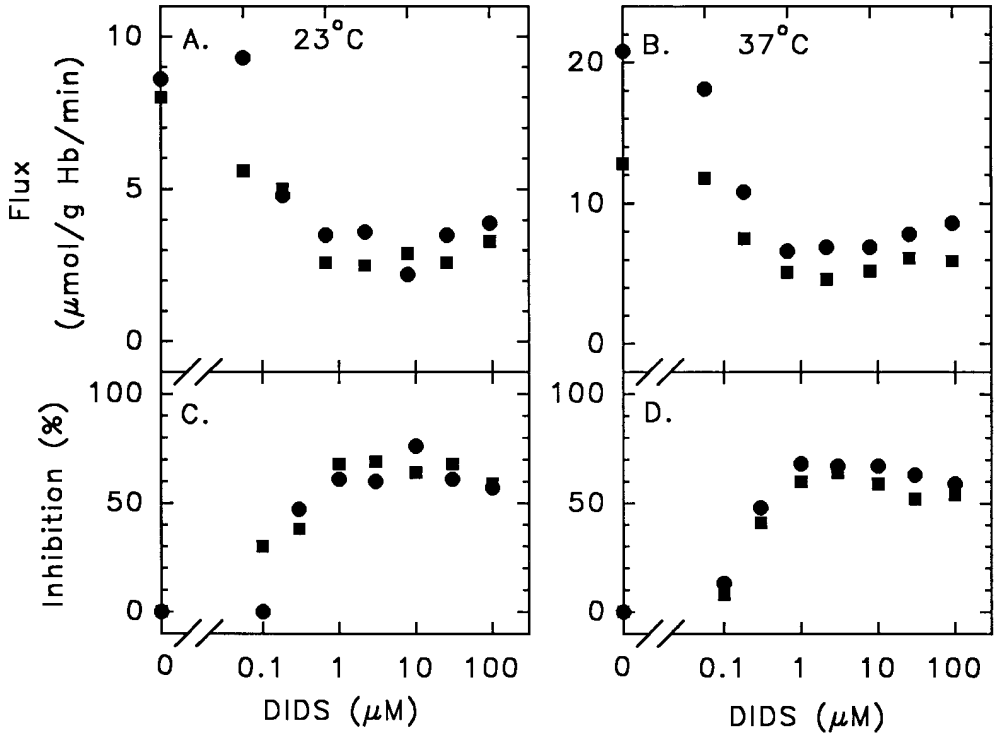

FIGURE 3. Effect of varied [DIDS] on valinomycin-induced net efflux (*A* and *B*) of K^+ (*circles*) and Cl^- (*squares*), and on the percent inhibition of the net effluxes (*C* and *D*) at 23°C (*A* and *C*) and at 37°C (*B* and *D*). Washed cells were suspended at 1.2% hematocrit in medium containing 1 mM KCl, 149 mM NaCl, and 10 mM HEPES buffer, pH 7.4, at either 25°C or at 37°C, and were pretreated with varied concentrations of DIDS for 30 min. Samples were removed before and 10 min after addition of 3 μM valinomycin. The centrifugally packed cells were analyzed for K^+, Cl−, and hemoglobin, and the net effluxes were determined by the cold-quench method (see MATERIALS AND METHODS and Freedman et al., 1994).

If band 3 had different chloride conductances with reversibly and irreversibly bound DIDS, with complex I showing greater inhibition than complex II, the partial inhibition by DIDS could be a consequence of the irreversible reaction of the inhibitor with the transport protein. From the activation energy for irreversible binding determined by Janas et al. (1984), the halftime of the covalent reaction is 3.6 min at 23°C and 0.46 min at 37°C; thus, the preincubation of 30 min with DIDS that we used would be sufficient to ensure complete irreversible binding. To determine whether or not the duration of exposure to DIDS influences the existence of the DIDS-insensitive efflux, valinomycin was added 1 min (Fig. 4, *circles*) or 30 min (Fig. 4, *squares*) after DIDS, and the fluxes were determined in duplicate (*filled and hollow symbols*) in the continued presence of DIDS, either at 23°C (Fig. 4 *A*) or at 37°C (Fig. 4 *B*). The average fluxes in the duplicate suspensions for 1

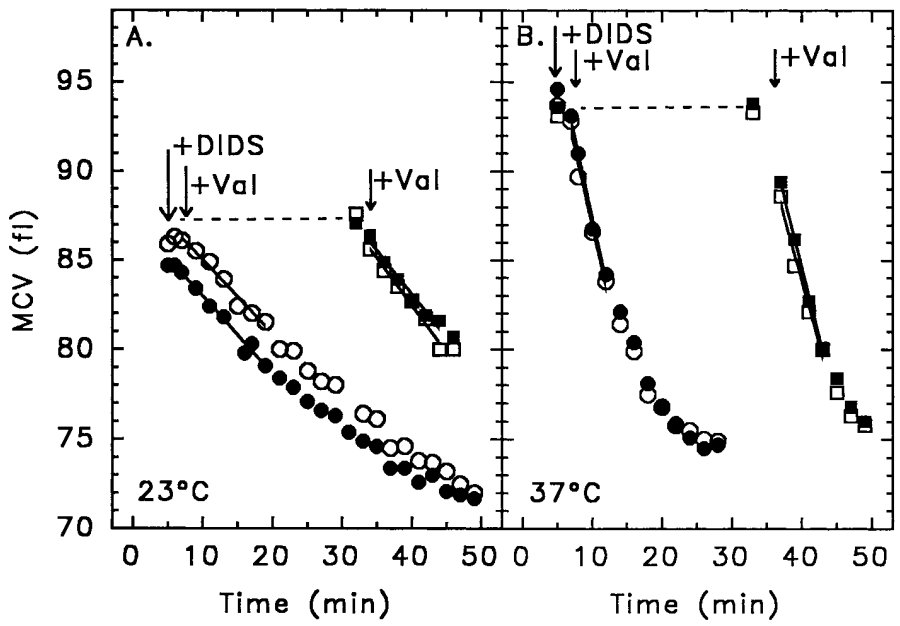

FIGURE 4. Effect of duration of preincubation with DIDS on valinomycin-induced net efflux at 23°C (*A*) and at 37°C (*B*). Washed cells at 1.2 percent hematocrit in medium containing 1 mM KCl and 149 mM NaCl were pretreated with 10 μM DIDS for either 1 min (*circles*) or 30 min (*squares*), followed by addition of 3 μM valinomycin (at *arrows*), and the mean cell volume (MCV) was determined (see MATERIALS AND METHODS) in duplicate suspensions (*filled and hollow symbols*) at the indicated times.

Published February 1, 1997

min exposure to DIDS were within 20% of those determined for 30 min exposure to DIDS, and thus the DIDS-insensitive flux persists with a brief exposure as well as for complete irreversible binding.

Current-Voltage and Conductance-Voltage Curves

Current-voltage curves for DIDS-insensitive chloride conductance were determined in five experiments, for which the mean initial cell K^+ and hemoglobin concentrations, cell water content, Donnan ratio and membrane potential are given in Table I. The current-voltage curves from two experiments, which were shown previously (Fig. 8 in Freedman et al., 1994), and from three additional experiments, are all shown together in Fig. 5 *A*, and also in Fig. 5 *C*. The data points from experiments with valinomycin at 1 μM (*filled circles and squares*) or at 3 μM (*filled triangles*), or with gramicidin at 60 ng/ml (*hollow circles and squares*) all fall closely about the same curve. The solid lines are the best-fit predictions of the voltage-gated mechanism of transport (Fig. 5 *A*) or the single barrier model (Fig. 5 *B*), as discussed below. The slopes between adjacent points represent the chloride slope conductance, g_{Cl}, in accordance with the relation $g_{Cl} = di_{Cl}/d(E_m - E_{Cl})$. The measured slope conductances from each of the five experiments are shown in the conductance-voltage plots in Fig. 5, *B* and *D*, in which it is seen that the slope conductance increases from a value of 0.015 ± 0.005 S/g Hb (SD, $n = 5$) near the reversal potential where $E_m = E_{Cl}$, to a maximal value of 0.055 ± 0.005 (SD, $n = 5$) at hyperpolarizing voltages, representing a fourfold increase ($P < 0.001$, paired Student's t test). The significant fourfold increase in slope conductance at hyperpolarizing voltages (Fig. 5 *B*) implies that the current-voltage plot in Fig. 5 *A* is superlinear; if the current-voltage plot (Fig. 5 *A*) were linear, then the slope conductances in Fig. 5 *B* would have been constant at varied voltage, in contrast to the results. The solid line in Fig. 5 *D* represents the best fit to a single barrier model, as discussed below, and the solid line in Fig. 5 *B* represents the best fit to a Boltzmann distribution of gating charge, according to which half the channels are open at −27 ± 2 mV, with an equivalent gating charge of −1.2 ± 0.3, also as discussed below.

TABLE I

Initial Cell Potassium and Hemoglobin Concentrations, Water Content, Donnan Ratio and Membrane Potential, and Constant Field K^+ and Cl^- Permeabilities of Human Red Blood Cells Treated with Valinomycin or Gramicidin

Cell potassium, $[K^+]_c$ (mM)	130 ± 4 (3%)	
Hemoglobin (g/ml cell water)	0.44 ± 0.02 (5%)	
Cell water (g/g cells)	0.662 ± 0.009 (1%)	
Donnan ratio, r_{cl}	0.67 ± 0.02 (4%)	
Membrane potential, E_{cl} (mV)	−10 ± 0.9 (9%)	
Constant field permeabilites	P_K/P_{Cl}	P_{Cl} (h^{-1})
−DIDS	20	0.49
+DIDS	74 ± 9	0.13

The values for cell K^+, hemoglobin, water content, Donnan ratio, and membrane potential are corrected for trapped medium (see MATERIALS AND METHODS) and are means ± SD for five donors; coefficients of variation are in parentheses. The value of P_K/P_{Cl} without DIDS is from Freedman and Hoffman (1979*b*); the value with DIDS is from Fig. 6 *C* (*middle line*). The value of P_{Cl} with DIDS is from Fig. 6 *A* (*lower line*); the value without DIDS was deduced as described in the text.

Comparison of Data with Electrodiffusion, Barrier, and Voltage-gated Mechanisms

We next show that in human red blood cells treated with valinomycin or gramicidin, the inward rectifying DIDS-insensitive Cl^- conductance (Fig. 5 *A*) is inconsistent with electrodiffusion through pores that are always open (Fig. 7, *lower left quadrant*). Moreover, the magnitude of the increase in conductance at hyperpolarizing voltages is quantitatively inconsistent with single-occupancy multiple barrier models (Läuger, 1973) that have described nonlinear ion currents through gramicidin channels. In contrast, the data are well described either by a single barrier model (Fig. 5, *C* and *D*, *solid lines*) or by a voltage-gated mechanism (Fig. 5, *A* and *B*, *solid lines*).

Predictions of an Electrodiffusion Mechanism. Because the theory of electrodiffusion (Goldman, 1943; Hodgkin and Katz, 1949; for discussion see Silver, 1985) predicts rectifying nonlinear current-voltage curves when the concentrations of internal and external permeant ions are unequal, we evaluated whether or not the experimentally determined inward rectifying DIDS-insensitive current-voltage curve for Cl^- (Fig. 5 *A*) is compatible with an electrodiffusion mechanism. To understand the current-voltage curves predicted according to the theory of electrodiffusion, as applied to the present experimental conditions, it is helpful to examine each of the following measured parameters at varied $[K^+]_o$: (*1*) the membrane potential E_m (Fig. 6 *C*, *middle line*); (*2*) the equilibrium potentials $E_K = -(RT/\mathcal{F})\ln[K^+]_c/[K^+]_o$ and $E_{Cl} = (RT/\mathcal{F})\ln[Cl^-]_c/[Cl^-]_o$ (Fig. 6 *C*, *lower and upper lines*, respectively); (*3*) the driving forces, $E_m - E_{Cl}$ and $E_m - E_K$ (Fig. 6 *B*); and (*4*) the ionic currents, i_K and i_{Cl} (Fig. 6 *A*).

With an electrodiffusion mechanism, the membrane potential E_m for human red blood cells treated with the K^+ ionophore valinomycin, or with gramicidin in sodium-free choline medium, is given by the Goldman-Hodgkin-Katz equation as follows:

$$E_m = -\frac{RT}{\mathcal{F}}\ln\frac{P_K[K^+]_c + P_{Cl}[Cl^-]_o}{P_K[K^+]_o + P_{Cl}[Cl^-]_c} \quad (1)$$

where P_K and P_{Cl} are the constant field permeabilities (s^{-1}) and $RT/\mathcal{F}$ is 25.5 mV at 23°C. Alternatively, with

Published February 1, 1997

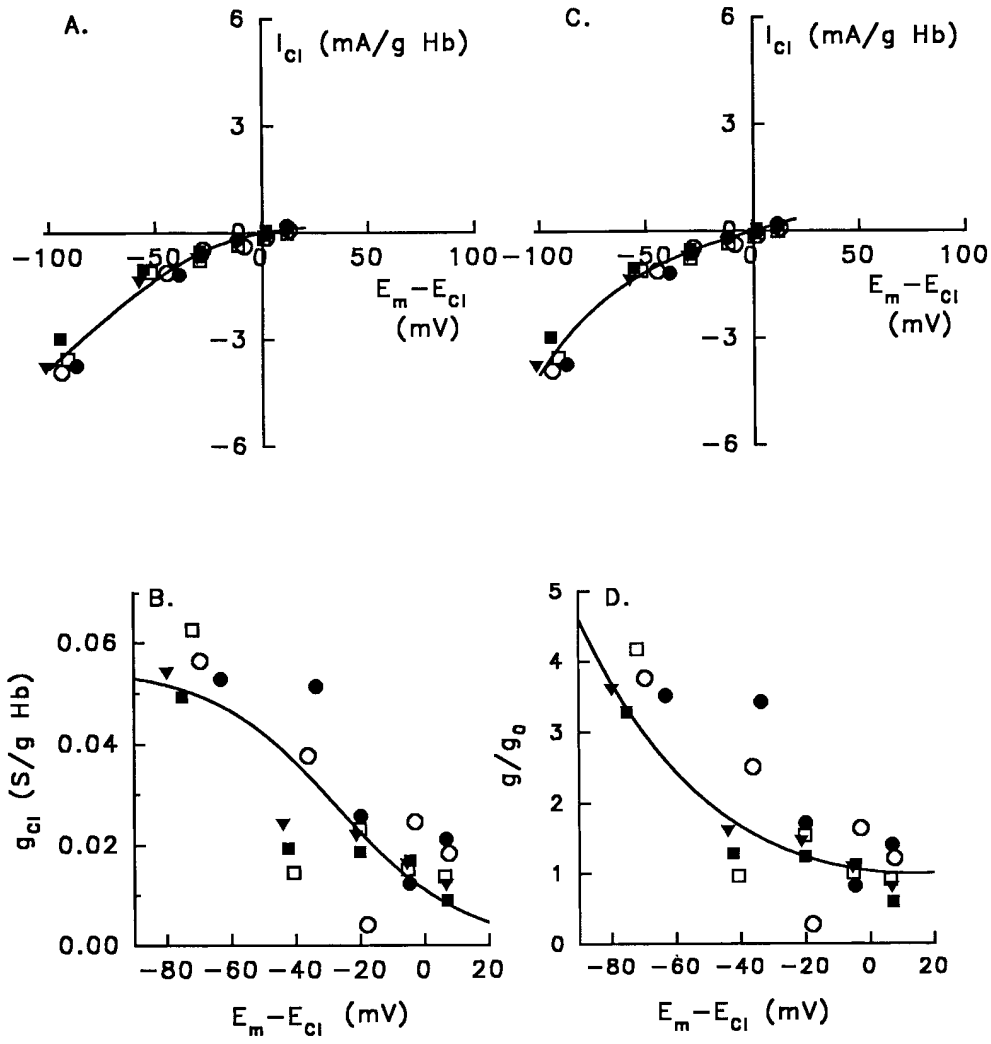

FIGURE 5. Current-voltage curves (*A* and *C*) and conductance-voltage curves (*B* and *D*) for five experiments (represented by different symbols) with human red blood cells treated with 10 μM DIDS (pH 7.5, 23°C), determined as described in MATERIALS AND METHODS. Solid lines represent best fits of the voltage-gated mechanism of transport (*A* and *B*) and the single barrier model (*C* and *D*) to the same set of experiments. The five experiments (each with six different concentrations of $[K^+]_o$) were as follows: two experiments with 1 μM valinomycin (*filled circles and squares*); one experiment with 3 μM valinomycin (*filled triangles*), and two experiments with 60 ng/ml gramicidin in choline medium (*hollow circles and squares*). Each data point in *B* and *D* represents the slope conductance between adjacent data points in *A* from the same experiment, and is plotted at the midpoint of the voltage for each pair of data points. The solid lines in *C* and *D* represent best fits of the single barrier model to the data, according to Eq. 5 for *C* and Eq. 7 for *D* (see text), with $\gamma = 0.43 \pm 0.02$. The solid lines in *A* and *B* represent best fits of the voltage-gated mechanism of transport, according to Eq. 14 for *A* and Eq. 12 for *B* (see text). For this mechanism, the maximal conductance, $g_{max} = 0.055 \pm 0.005$ *S/g Hb* (SD, $n = 5$), was taken from the measured slopes between −50 and −100 mV, corresponding to 10 and 1 mM $[K^+]_o$, in each experiment. From the curve fits, the voltage E_o giving half-maximal conductance is -27 ± 2 mV, and the equivalent gating charge z_G is -1.2 ± 0.3.

$i_K = g_K(E_m - E_K)$, and $i_{Cl} = g_{Cl}(E_m - E_{Cl})$, then for $i_K = -i_{Cl}$, it follows that E_m (Fig. 6 *C, filled circles and middle line*) is the conductance-weighted average of E_K (Fig. 6 *C, bottom line*) and E_{Cl} (Fig. 6 *C, top line*):

$$E_m = \frac{g_K}{g_K + g_{Cl}} E_K + \frac{g_{Cl}}{g_K + g_{Cl}} E_{Cl}. \quad (2)$$

The data points in Fig. 6 *C* represent the average values of E_m at each value of $[K^+]_o$ from the same five experiments (i.e., the values from the absissa of Fig. 5 but without subtracting E_{Cl}); the solid line through the data is the best fit of Eq. 1, according to which the ratio $\alpha = P_K/P_{Cl} = 74 \pm 9$.

Defining the inhibition I by DIDS of P_{Cl} as $I = (P_{Cl}^o - P_{Cl})/P_{Cl}^o$, where P_{Cl}^o is the uninhibited constant field permeability to Cl^-, it follows that $I = 1 - (\alpha^o/\alpha)$. From the fluorescence of diO-C_6(3), as reported by Hoffman and Laris (1974), we previously estimated the uninhibited ratio $\alpha^o = P_K/P_{Cl}^o$ in valinomycin-treated red cells to be 20 ± 5 at pH 7.4 and 23°C (Freedman and Hoffman, 1979*b*), in agreement with the value of 17 at pH 7.3 and 20°C determined from the partitioning of diS-C_3(5) (Hladky and Rink, 1976), and also in agreement with the value of 18 at pH 7.4 and 37°C determined from constant field analysis of ^{42}K fluxes (Hunter, 1977). Thus, $I = 1 - (20/74) = 0.73$, or 73% inhibition of P_{Cl} by 10 μM DIDS at 23°C, in good agreement with the value of 72 ± 8 ($n = 2$) percent inhibition of P_{Cl} with 10 μM DIDS at pH 7.04 and 37°C determined by Knauf et al. (1983) by a different method.

The driving forces $E_m - E_{Cl}$ (Fig. 6 *B, circles*) and $E_m - E_K$ (Fig. 6 *B, squares*) were also calculated from the mea-

Published February 1, 1997

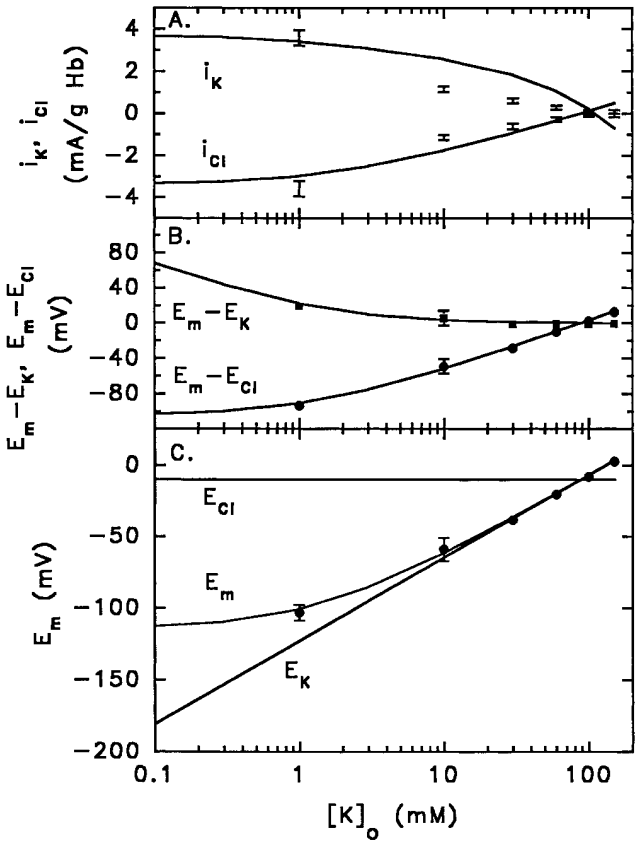

FIGURE 6. Comparison of measured currents and voltages with predictions of the theory of electrodiffusion, as applied to human red blood cells at varied $[K^+]_o$, first treated with 10 μM DIDS, and then with valinomycin or gramicidin (in sodium-free medium). Data points represent the means ± 1 SD of the measured values at each $[K^+]_o$ of (*A*) i_K and i_{Cl}, (*B*) $E_m - E_K$ and $E_m - E_{Cl}$, and (*C*) E_m itself from the same five experiments shown in Fig. 5. (*A*) Ionic currents i_K (*upper line* is the best-fit according to Eq. 3) and i_{Cl} (*lower line* is the best-fit according to Eq. 4). From Eq. 4 for i_{Cl} and the measured values of E_m (Fig. 6 *C*), the best-fit value of P_{Cl} is 3.7 ± 0.4 (10^{-5}) s^{-1}, or 0.13 h^{-1}; using $\alpha = P_K/P_{Cl} = 74$ (Fig. 6 *C*), the value of P_K is 2.7 (10^{-3}) s^{-1}, or 9.7 h^{-1}. (*B*) Driving forces $E_m - E_K$ (*upper line*) and $E_m - E_{Cl}$ (*lower line*), taking E_m from Fig. 6 *C*, E_K from the measured cell K^+ (Table I), and E_{Cl} from the measured Donnan ratio for Cl^- (Table I). (*C*) Membrane potential E_m (*middle line*) in relation to E_K (*lower line*) and E_{Cl} (*upper line*); from Eq. 1, the best-fit value of P_K/P_{Cl} is 74 ± 9. Calculations (*solid lines*) used $[K^+]_c$ = 130 mM, E_{Cl} = −10 mV with $[Cl^-]_c$ = 101 mM and $[Cl^-]_o$ = 150 mM corresponding to r_{Cl} = 0.67 (from Table I).

sured values of E_m (Fig. 6 *C*, *circles*), and from the measured values of E_K and E_{Cl} (see MATERIALS AND METHODS). The solid lines in Fig. 6 *B* were calculated versus $[K^+]_o$ using Eq. 1 with the value of P_K/P_{Cl} = 74, and are seen to fit the measured driving forces. Thus, the theory of electrodiffusion describes adequately the measured membrane potentials (Fig. 6 *C*) and the driving forces (Fig. 6 *B*).

The measured currents i_K and i_{Cl} (mA/g Hb) from the five experiments are shown plus and minus their standard deviations in Fig. 6 *A*; the solid lines were computed from the theory of electrodiffusion as follows:

$$i_K = \beta P_K \mathcal{F}\phi \frac{[K^+]_c - [K^+]_o e^{-\phi}}{1 - e^{-\phi}}, \quad (3)$$

$$i_{Cl} = -\beta P_{Cl} \mathcal{F}\phi \frac{[Cl^-]_c - [Cl^-]_o e^{\phi}}{e^{\phi} - 1}, \quad (4)$$

where $\mathcal{F}$ = 96,490 coul/eq, φ is the reduced potential $\mathcal{F}E_m/RT$, and the factor β = 2.11 (10^{-3}) liter H_20/g Hb = (0.717 liter H_20/liter cells)/(340 g Hb/liter cells) converts the units of current from mA/liter H_2O to mA/g Hb. The best fit of Eq. 4 to the DIDS-insensitive Cl^- current, using the measured values of E_m, is obtained with a value of P_{Cl} = 3.7 ± 0.4 (10^{-5}) s^{-1}, or 0.13 h^{-1} (Table I). The upper solid line in Fig. 6 *A* was computed using this value of P_{Cl} and the ratio α = 74, corresponding to P_K = 2.7 (10^{-3}) s^{-1}, or 9.9 h^{-1}. The uninhibited constant field Cl^- permeability may be obtained from $P_{Cl}^o = P_{Cl}/(1\text{-}I)$ = 1.4 (10^{-4}) s^{-1}, or 0.49 h^{-1} (Table I). Hunter (1971, 1977) reported a constant field P_{Cl} of 0.036 min^{-1} (*n* = 7, pH 7.4, 37°C), corresponding to 2.2 h^{-1}, with a Q_{10} of about three and an activation energy between 14°C and 37°C of 16.4 kcal/mol, from which we estimate his P_{Cl} at 23°C to be 0.63 h^{-1}, in close agreement with what we find. A comparable value of 0.033 min^{-1}, or 2.0 h^{-1} (*n* = 7, pH 7.1, 37°C) was reported by Knauf et al. (1977). A value of 0.06 min^{-1}, or 3.6 h^{-1} (pH 7.8, 25°C), some sevenfold higher than what we find, was estimated by Fröhlich et al. (1983), and values of 0.055 and 0.061 min^{-1} (pH_c 7.2, 37°C), or 3.3 and 3.7 h^{-1}, were reported by Bennekou and Stampe (1988).

Whereas the theory of electrodiffusion adequately describes the voltages (Fig. 6 *C*) and the driving forces (Fig. 6 *B*), the predicted currents (Fig. 6 *A*, *solid lines*) lie outside of the standard deviations of the data. As $[K^+]_o$ is decreased, the slope between the measured currents is either constant or increases monotonically (Fig. 6 *A*, *data*), whereas the predicted slopes of the best fit lines decrease monotonically (Fig. 6 *A*, *solid lines*). The disparity between the theory of electrodiffusion and the currents is even more apparent when the currents are plotted against the driving forces in the current-voltage curve, as seen by comparing the data in Fig. 5 *A* with the predictions in Fig. 7. The predicted current-voltage curves in Fig. 7 were calculated for values of $\alpha = P_K/P_{Cl}$ of 20, 40, and 200, corresponding to 0, 50, and 90 percent inhibition of P_{Cl}, respectively. Examination of Fig. 7 reveals that the theory of electrodiffusion predicts linear[2] current-voltage curves for Cl^- between 0 and 90% inhibition of P_{Cl} (*lower left quad-*

[2]Due to the inward Cl^- concentration gradient, electrodiffusion actually predicts a very slight outward rectification of Cl^- current, as would be apparent over an extended range of voltage.

Published February 1, 1997

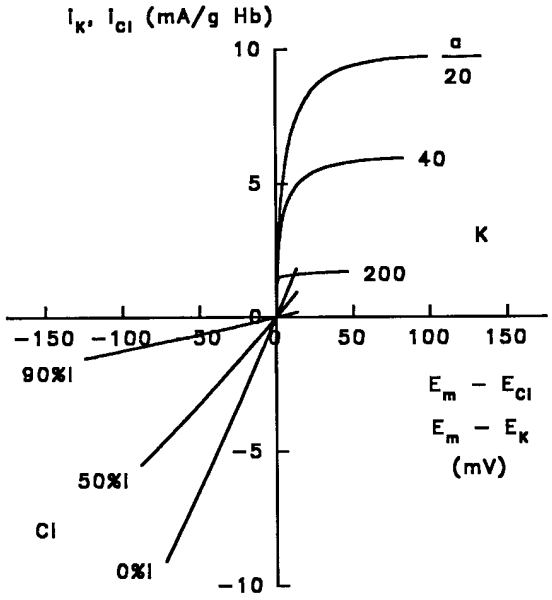

FIGURE 7. Predicted current-voltage curves, according to the theory of electrodiffusion, with 0%, 50%, and 90% inhibition by DIDS, corresponding to P_K/P_{Cl} = 20, 40, and 200, respectively. The upper right quadrant shows the predicted potassium currents, i_K, plotted vs $E_m - E_K$, calculated as for the upper lines in Fig. 6, *A* and *B*; the lower left quadrant shows the predicted chloride currents, i_{Cl}, calculated as for the lower lines in Fig. 6, *A* and *B*.

rant), but sublinear current-voltage curves for K^+ (*upper right quadrant*). Clearly, the finding of an inward rectifying current-voltage curve for Cl^- (Fig. 5 *A*) is inconsistent with the predictions of electrodiffusion (Fig. 7). If Eq. 4 is used to calculate P_{Cl} from the measured currents and voltages at each $[K^+]_o$, then the data are described if P_{Cl} (hr^{-1}) is assumed to increase linearly with hyperpolarizing voltages, between 0 and −100 mV, according to $P_{Cl} = -0.0010E_m + 0.05$. The voltage dependence of DIDS-insensitive Cl^- permeability could be due either to an effect of voltage on ion permeation over a barrier, or alternatively, to an effect of voltage on channel gates, as evaluated below.

The explanation for the prediction of electrodiffusion theory that the current-voltage curves are nearly linear for Cl− but sublinear for K^+ (Fig. 7) is found by examining the membrane potential, the driving forces, and the currents (Fig. 6). As $[K^+]_o$ is decreased at constant $[Cl]_o$ and constant E_{Cl}, the membrane potential increasingly hyperpolarizes upon addition of K^+ ionophores (Fig. 6 *C*), thus increasing the outward driving force, $E_m - E_{Cl}$, for Cl^- (Fig. 6 *B*, *lower line*). The inside negative voltage thus drives an outward Cl^- efflux, or inward current i_{Cl} (Fig. 6 *A*, *lower line*), which parallels the increased negative driving force (Fig. 6 *B*, *lower line*). Thus, chloride conductance g_{Cl} is nearly constant, and the predicted current-voltage curves for Cl^- are nearly linear (Fig. 7, *lower left quadrant*). Considering potassium, the effect of decreased $[K^+]_o$ is greater on E_K than on E_m as both become more negative (Fig. 6 *C*, *lower two lines*), resulting in an increased positive driving force $E_m - E_K$ (Fig. 6 *B*, *upper line*), which drives the efflux of K^+. Decreasing $[K^+]_o$, however, increases the outward concentration gradient for efflux of K^+, but simultaneously creates a negative electrical potential which impedes the efflux. Thus, the predicted potassium current, i_K, tends to plateau (Fig. 6 *A*, *upper line*) while the driving force, $E_m - E_K$, continues to increase (Fig. 6 *B*, *upper line*), resulting in a predicted voltage-dependent potassium conductance g_K and sublinear current-voltage curves for K^+ (Fig. 7, *upper right quadrant*). The data for K^+, however, were restricted to only a 25-mV range of $E_m - E_K$ (Fig. 6 *B*), and the corresponding measured current-voltage curves (not shown) were thereby unsuitable for comparison with the predictions of the complex mechanisms of ion permeation described for the ionophore valinomycin (Läuger and Stark, 1970; Stark and Benz, 1971), or for the channel-forming antibiotic gramicidin (Läuger, 1973; Andersen, 1983*a*, *b*).

Predictions of a Single Barrier Model. For a single barrier located at a fractional distance γl from the intracellular side of a membrane of thickness l ($0 \le \gamma \le 1$), separating an intracellular solution of concentration c_1 from an extracellular solution of concentration c_2, the theory of absolute reaction rates predicts the following current-voltage relationship (Jack et al., 1983):

$$I = K[c_2 e^{-z(\gamma-1)\phi)} - c_1 e^{-z\gamma\phi)}], \quad (5)$$

where $K = z\mathcal{F}A \exp(-\Delta G_o/RT)$, z is the ionic valence, ΔG_o is the free energy height of the barrier in the absence of a voltage, and ϕ is the reduced potential $\mathcal{F}E_m/RT$. For a centrally located barrier ($\gamma = \frac{1}{2}$) with symmetric solutions ($c_1 = c_2$), the current-voltage relationship simplifies to

$$I = 2K'\sinh(z\phi/2), \quad (6)$$

where $K' = cK$.

From Eq. 5, the slope conductance g, relative to that at zero voltage g_0, is given by

$$\frac{g}{g_0} = \frac{(c_2/c_1)(\gamma-1)e^{-z(\gamma-1)\phi} - \gamma e^{-z\gamma\phi}}{(c_2/c_1)(\gamma-1) - \gamma}. \quad (7)$$

Fitting Eq. 7 to the conductance-voltage data in Fig. 5 *D* yields a best-fit value of γ of 0.43 ± 0.02. Using this value for γ, a value of $K = 0.0033 \pm 0.0001$ is obtained from a fit of Eq. 5 to the data in Fig. 5 *C*. Thus, we conclude that a single barrier located near the center of the transmembrane electric field is consistent with the nonlinear conductance-voltage and current-voltage curves for DIDS-insensitive Cl^- conductance. Moreover, in the context of the generalized Nernst-Planck electrodiffu-

Published February 1, 1997

sion theory (Neumke and Läuger, 1969), which is an alternative to absolute reaction rate theory but which also takes into account the existence of a membrane barrier, the shape of the barrier, as well as its location, can also influence the degree of rectification (Hall et al., 1973).

Predictions of Multiple Barrier Models. Applying the theory of absolute reaction rates to ion transport through pores with multiple barriers, Läuger (1973) calculated the slope conductance g as a function of voltage V, relative to the limiting conductance at zero voltage g_0, for single-occupancy channels for the specialized case in which the multiple internal barriers have equal heights.

At low salt concentrations ($c \approx 0$),

$$\frac{g}{g_0} = \frac{q^{1/2}(q-1)(q^n-1/q)[2k_i+(n-1)k_{pa}]/z\phi}{(q-1)(q^n+1)k_i+(q^n-q)k_{pa}} \quad (8)$$

and at high salt concentrations[3] ($c \to \infty$),

$$\frac{g}{g_0} = \frac{nq^{1/2}(q-1)(q^n-1/q)[2k_i+(n-1)k_{pa}]/z\phi,}{(q+1)(q^n-1)k_i+[(n-1)q(q^n-1/q)-(q^n-q)]k_{pa}} \quad (9)$$

where $q = e^{z\phi/(n+1)}$, ϕ is the reduced potential ($\mathcal{F}V/RT$), z is the ionic valence, n is the number of barriers, and k_i and k_{pa} are the rate constants for an ion jumping over the internal and surface barriers, respectively. For the case of $n = 9$, with the ratio of k_i/k_{pa} ranging from zero to infinity, Läuger (1973) (his Fig. 3) showed that at low ion concentrations ($c \approx 0$) sublinear current-voltage curves are predicted when the surface barriers are rate-limiting, with superlinear current-voltage curves predicted when the internal barriers are rate-limiting. At high ion concentrations ($c \to \infty$), the predicted current-voltage curves are nearly linear if the internal barriers are rate-limiting, and slightly superlinear when the surface barriers are rate-limiting. For the conditions in which superlinear current-voltage curves are predicted by single-occupancy multiple barrier models, the extent of the predicted increase in conductance at 100 mV is only 10–20% greater than at 0 mV, far less than the fourfold increase seen for DIDS-insensitive Cl^- conductance over the same range of voltage (Fig. 5). An extension of these model calculations, based on Eqs. 8 and 9, showing the relative conductance at −100 mV, relative to that at 0 mV, for n ranging from 2 to 10 is shown in Fig. 8. The calculations show that at high salt concentration, g/g_0 is always within 20% of unity (Fig. 8 *B*), and at low salt concentration g/g_0 is within a factor of 2 of unity (Fig. 8 *A*). Thus, single-occupancy multiple barriers have insufficient rectification to explain the fourfold increase of conductance seen for DIDS-insensitive Cl^- conductance.

A multiple occupancy channel could have a steeper voltage dependence of conductance if a second ion blocked the transport of the first ion, and if the second ion exhibited voltage-dependent binding. Fluctuating barrier models could also give rise to a steep voltage dependency if an electrically charged part of the transport protein crossed the transmembrane electric field during channel gating. Both of these types of barrier models could be viewed as examples of voltage-gated

[3] In Läuger (1973), Eq. 58 contains a typographical error. The equation given for g/g_0 at high salt has the wrong limiting behavior at $V = 0$ and does not produce the graph of g/g_0 vs voltage shown in his Fig. 3 *B*; the modification in Eq. 9 above produces the plots in Läuger's Fig. 3 *B*.

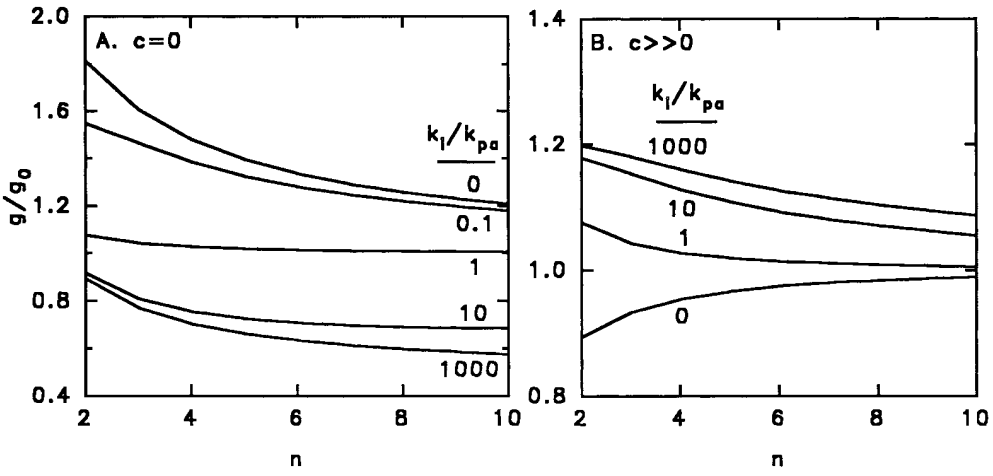

FIGURE 8. Predicted relative slope conductance g/g_o at −100 mV (relative to zero mV) for a single occupancy pore containing multiple internal barriers of equal height plotted as a function of the number n of barriers in the pore. *A* and *B* are the predictions for low ($c \approx 0$) and high ($c \to \infty$) salt concentrations according to Eqs. 8 and 9, respectively, based on absolute reaction rate theory. The ratio k_i/k_{pa} represents the rate constant for an ion hopping over an internal barrier, relative to the rate constant for hopping over a surface barrier.

Published February 1, 1997

mechanisms, the gating being effected either by an ion or by part of the protein.

Predictions of a Voltage-gated Mechanism. We next tested the consistency of the data with a voltage-gated mechanism (Hodgkin and Huxley, 1952; for discussion see Hille, 1992). For a population of channels whose open (O) and closed (C) states are controlled by gates with charge z, if the charged gates distribute across the transmembrane electric field in accordance with a Boltzmann distribution, then

$$\frac{O}{C} = e^{z(E_m - E_o)/24}, \quad (10)$$

where $kT/e = 24$, E_m is the transmembrane electrical potential, and E_o is the voltage at which half the channels are open.

The open state probability, P_o, is given by

$$P_o = \frac{O}{C+O} = \frac{1}{1 + e^{-z(E_m - E_o)/24}}, \quad (11)$$

For simplicity, this treatment assumes a single closed state rather than multiple states (see Bezanilla, 1994, for review). Note that the limit of $(d\ln P_o/dE)$ as E_m approaches minus infinity is ze/kT, or z/24, so that z is 24 divided by the change in voltage for an e-fold increase in F (Hille, 1992). Since the conductance, g, is proportional to the open state probability, or $P_o = g/g_{max}$, then

$$g = \frac{g_{max}}{1 + e^{-z(E_m - E_o)/24}}. \quad (12)$$

A satisfactory fit of Eq. 12 to the measured Cl^- conductances as a function of varied E_m is shown in Fig. 5 *B* (*solid line*), with the best-fit parameters given in the RESULTS. To derive an expression for the current-voltage curve itself, the conductance-voltage expression, $g(E) = di(E)/dE$, was integrated as follows:

$$\int_0^i di = \int_0^{E_m} g(E)\,dE = \int_0^{E_m} \frac{g_{max}}{1 + e^{-z(E - E_o)/24}} dE. \quad (13)$$

Integration results in the following expression for the current-voltage curve:

$$i = g_{max}\left[E_m + \frac{24}{z}\ln\frac{1 + e^{-z(E_m - E_o)/24}}{1 + e^{zE_o/24}}\right]. \quad (14)$$

The solid line in Fig. 5 *A* is the best-fit of Eq. 14 to the experimental data with the parameters given in RESULTS. Clearly, the voltage-gated mechanism with a Boltzmann distribution of gating charge is also consistent with the inward rectifying conductance-voltage and current-voltage curves characterizing DIDS-insensitive Cl^- transport; the percentage deviation between the predicted and observed Cl^- currents is threefold less with the voltage-gated mechanism than for the theory of electrodiffusion. The derived value for the gating charge of -1.2 ± 0.3 represents an equivalent value and a lower limit since more charges could distribute across a smaller portion of the transmembrane electric field.

DISCUSSION

The most significant conclusion from this analysis of our data on DIDS-insensitive Cl^- conductance is that an electrodiffusion mechanism, and single occupancy multiple barrier models, are quantitatively inconsistent with the inward rectifying current-voltage curve for Cl^-, whereas either a single barrier or, alternatively, a voltage-gated mechanism involving a Boltzmann distribution of negative gating charge across the transmembrane electric field are consistent with the experimental results. An important aspect of the gating charge mechanism is that the negative gating charge is mobile. A gating mechanism could involve a gating charge on the channel itself, or alternatively, a voltage-dependent block by some ionic gating particle (see chapter 18 in Hille, 1992).

The theory of electrodiffusion assumes that the ionic currents are independent, that the membrane is symmetrical, that the transmembrane electric field is constant, and that ions first partition into the membrane and then diffuse across, driven by concentration and electrical gradients (Goldman, 1943; Hodgkin and Katz, 1949). This theory specifically predicts the dependence on ion concentrations of the transmembrane electrical potential (Eq. 1 and Fig. 6 *C*, *middle solid line*) and the ionic currents (Eqs. 3–4 and Fig. 6 *A*, *solid lines*), and also predicts the relationship of current to voltage (Eqs. 3–4, with E_m taken from Eq. 1, and Fig. 7). Interestingly, and in contrast, barrier models and the voltage-gated mechanism predict the dependence on voltage of conductance (Eqs. 7–9 and 12, and Figs. 5, *B* and *D*, *solid lines*), and of current (Eqs. 5 and 14, and Fig. 5, *A* and *C*, *solid lines*), independently of the relationship between voltage and ion concentration. With a voltage-gated mechanism, the maximal conductance, g_{max}, would itself depend on ion concentrations in accordance with the specific heights of electrical barriers and the depths of wells, and their locations within the membrane. Remarkably, the postulation of a voltage-gated process per se permits the prediction of an inward rectifying current-voltage curve (Eq. 14, and Fig. 5 *A*, *solid line*) without knowledge of the mechanism of ion permeation when the gate is open. The finding of an inward rectifying DIDS-insensitive Cl^- current (Fig. 5 *A*) with moderate voltage-dependency thus excludes nongated electrodiffusion (Fig. 7) and single occupancy multiple barrier models, but does not rule out the possibilities that Cl^- crosses the membrane by hop-

Published February 1, 1997

ping over a single barrier or via electrodiffusion when voltage-gated channels are open.

Prior estimates of the conductive Cl^- permeability of human red blood cells (Hunter, 1977; Knauf et al., 1977, Kaplan et al., 1983; Fröhlich et al., 1983) relied on the applicability of the constant field theory (Goldman, 1943; Hodgkin and Katz, 1949). Hunter (1977) originally considered his estimate of P_{Cl} to be "order of magnitude" because of the assumptions inherent in deriving the necessary equations relating voltage to ion concentrations (Eq. 1) and to ion fluxes (Eqs. 3–4). Instead of calculating membrane potentials theoretically, Bennekou and Christophersen (1986) estimated red cell membrane potentials from changes in the external pH of unbuffered suspensions in the presence of the proton ionophore CCCP, and inferred that the flux ratio for K^+ mediated by valinomycin is less than unity. If correct, this apparent contradiction with the assumption of independence would invalidate the use of the constant field theory for red cells treated with valinomycin, thus calling into question the validity and meaning of prior estimates of P_{Cl}. We also have evaluated the applicability of the constant field theory to red cells treated with valinomycin, first by calibrating optical potentiometric indicators to measure voltages (Freedman and Hoffman, 1979*b*; Freedman and Novak, 1983, 1984, 1987, 1989; Bifano et al., 1984; Freedman et al., 1988), and then by focusing on DIDS-insensitive Cl^- net fluxes with membrane potentials measured by means of FCCP (Freedman and Novak, 1987; Freedman et al., 1994). Our results for DIDS-treated cells show that the constant field theory (Eq. 1) precisely describes the relationship between membrane potential and $[K^+]_o$ (Fig. 6 *C*); the constant field theory also gives a reasonable numerical approximation to the K^+ and Cl^- currents (Fig. 6 *A*). From the change in the value of the ratio P_K/P_{Cl} with DIDS (from 20 to 74), we inferred the degree of inhibition of P_{Cl} by DIDS (73%). By fitting the measured Cl^- currents versus $[K^+]_o$ (Fig. 6 *A*), using the measured membrane potentials (Fig. 6 *C*), we estimated a value for the inhibited P_{Cl} ($0.13\ h^{-1}$), which together with the degree of inhibition, yields a value for the uninhibited P_{Cl} ($0.49\ h^{-1}$). Despite the reported deviation of the flux ratio from unity (Bennekou and Christophersen, 1986), our derived value for P_{Cl}, based on measured net fluxes and voltages, agrees remarkably well with previous estimates (Hunter, 1977; Knauf et al., 1977, 1983). Our analysis shows that Hunter's (1977) original estimate of P_{Cl} was considerably more accurate than realized at the time. The inward rectifying current-voltage curve for the DIDS-insensitive fraction of Cl^- net transport (Fig. 5), however, deviates markedly from the nearly linear curve predicted by the constant field theory (Fig. 7). A single barrier model (Eq. 5 and Fig. 5 *C*; Eq. 7 and Fig. 5 *D*) and a voltage-gated mechanism (Eq. 14 and Fig. 5 *A*; Eq. 12 and Fig. 5 *B*) are both consistent with the available experimental data. Examination of the predicted conductance-voltage plots (Figs. 5, *B* and *D*) suggests that extension of the voltage range in further experiments could allow discrimination between the two-state voltage-gating mechanism and rectification produced by a single barrier.

Two-dimensional arrays of the membrane domain of capnophorin have been reconstituted with lipids and crystallized (Wang et al., 1993, 1994; Reithmeier, 1993). Reconstructed images of the protein topography at 20 Å resolution indicate a dimeric structure with a cavity between the two monomers. ^{35}Cl nuclear magnetic resonance studies suggest that intracellular and extracellular hemichannels lead to the transport site of capnophorin (Falke and Chan, 1986*b*), and indicate that DIDS lies between the transport site and the extracellular medium, partially blocking the outward-facing transport site (Falke and Chan, 1986*a*). Earlier structure activity studies with a series of benzene sulfonic acid and stilbene disulfonates led to a proposed model of the DIDS-binding site that included juxtaposed positively charged groups providing electrostatic stabilization of the sulfonates on DIDS with adjacent hydrophobic and electron-donor centers (Barzilay et al., 1979). Fluorescence resonance energy transfer experiments indicate that the stilbene disulfonate-binding site is located only 34–42 Å from sulfhydryl reagents bound to cysteine residues on the 40,000-D amino-terminal cytoplasmic domain of capnophorin, consistent with DIDS residing in a cleft in the outer hemichannel (Rao et al., 1979). Moreover, substrate anions traverse only 10–15% of the transmembrane potential between the extracellular medium and the outward-facing transport site (Jennings et al., 1990), indicative of a low resistance for the outer hemichannel. With DIDS bound covalently in such a cavity, the possibility that the negatively charged sulfonic acid groups on the inhibitor could themselves traverse the transmembrane electric field and constitute the presumptive gating charge seems improbable, but cannot strictly be ruled out; further experiments with neutral inhibitors would be needed to resolve this question.

Further experiments should also be directed at resolving the question of whether covalently-bound DIDS partially blocks anion conductance mediated by capnophorin, or, alternatively, whether some other transport protein is responsible for DIDS-insensitive Cl^- conductance. DIDS-insensitive net efflux of Cl^- persists in the presence of 1 mM PCMBS (*p*-chloromercuribenzenesulfonate) (Knauf et al., 1983), a sulfhydryl reagent that inhibits the red cell monocarboxylate transport system (Deuticke et al., 1982). Moreover, lactate efflux is unaffected by extracellular Cl^- or sulfate (Deuticke et al., 1982). Both of these observations are inconsis-

Published February 1, 1997

tent with the lactate transporter mediating net Cl^- efflux. Chloride conductances that activate at hyperpolarizing voltages have been described in Aplysia neurons (Chesnoy-Marchais, 1983), in cultured mouse astrocytes (Nowak et al., 1987), and in rabbit urinary bladder (Hanrahan et al., 1985) and cortical collecting duct basolateral membranes (Sansom et al., 1990). A background chloride channel (denoted ClC-2), said to be "ubiquitously expressed" in epithelial and nonepithelial cells, is in the same gene family as Cl^- channels from *Torpedo* electroplax (ClC-0) and skeletal muscle (ClC-1). ClC-2 has a 3–5 pS single channel conductance and opens at negative voltages (Thiemann et al., 1992; Pusch and Jentsch, 1994); the voltage-gating is thus similar to DIDS-insensitive Cl^- conductance in human red blood cells (Fig. 5). Moreover, the inactivation gate of the double-barelled Cl^- channel from *Torpedo californica* (Miller and White, 1984) opens at hyperpolarizing voltages with an equivalent gating charge of -2.2 ± 0.1 (White and Miller, 1979), also similar to what we find in red cells.

As the concentration of DIDS is increased, the degree of inhibition of net Cl^- efflux is maximal at around 65% at 1 mM $[K^+]_o$ when the cells are pretreated with the inhibitor, and the valinomycin-induced fluxes are then measured in the continued presence of the inhibitor either at 23°C (Fig. 7 in Freedman et al., 1994) or at 37°C (Fig. 3). Assuming 0.34 g Hb/10^{10} cells, with each cell having a surface area of 133 μ^2, our value for the maximal DIDS-insensitive chloride conductance of 0.055 S/g Hb at 23°C corresponds to 1.4 $\mu S/cm^2$, in reasonable agreement with the value of 2.8 $\mu S/cm^2$ at the higher temperature of 37°C estimated from the data of Bennekou and Stampe (1988, their Fig. 4 and their Table II). The DIDS-insensitive conductive efflux of chloride characterized in the present study at hyperpolarizing voltages contrasts with the 99.999% inhibition by DIDS of the unidirectional efflux of Cl in the absence of ionophores at the normal resting potential of −9 mV (Gasbjerg et al., 1993); we previously reported that the degree of inhibition increases as the membrane potential becomes less negative (Freedman et al., 1994).

The results in Fig. 4 indicate that DIDS-insensitive conductance is largely unaffected ($\leq$20%) by whether DIDS is bound reversibly (1 min preincubation) or irreversibly (30 min preincubation). Circular dichroism spectra (Batenjany et al., 1993) and proteolytic digestion experiments (Kang et al., 1992) indicate that irreversible binding of DIDS changes the conformation of capnophorin to a more compact structure, possibly reflecting a conformational change that occurs during transport (Reithmeier, 1993).

After the cloning and sequencing of the murine cDNA coding for band 3 protein (AE1) by Kopito and Lodish (1985), the cDNA for the human red cell chloride transporter was also cloned and sequenced (Tanner et al., 1988; Lux et al., 1989; see Alper, 1991, for review). Band 3 protein has also been functionally expressed in *Xenopus laevis* toad oocytes microinjected with mRNA prepared from the cDNA clone from humans (Garcia and Lodish, 1989) and from mice (Bartel et al., 1989). Site-directed mutagenesis experiments with the mouse protein indicate that one of the isothiocyanate (NCS) groups on DIDS binds irreversibly to Lys-558 on the extracellular side of the 65-kD chymotryptic NH_2-terminal fragment with a stoichiometry of one inhibitor molecule per capnophorin monomer (Bartel et al., 1989; for review, see Passow et al., 1992).

The lock-carrier model for red cell anion transport proposed by Gunn (1978) included a titratable, positively charged transport site and a gating mechanism. The dependence on pH of Cl^- self-exchange in resealed ghosts (Funder and Wieth, 1976; Wieth and Bjerrum, 1982), and of sulfate fluxes in ghosts and intact cells (Schnell et al., 1977; Milanick and Gunn, 1984), indicated that the "carrier" could be singly or doubly protonated, and chemical labeling experiments with phenylglyoxal have implicated arginine residues in the mechanism of red cell anion transport (Wieth et al., 1982). Sulfate-chloride exchange normally includes a proton flux and is thereby electroneutral (Jennings, 1976), consistent with at least two positive charges and one negative charge at the transport site. When intact red cells are treated with Woodward's reagent K and borohydride (BH_4^-), glutamate 681 on human capnophorin is converted into an alcohol (Jennings and Smith, 1992), thus neutralizing its negative charge. Under these conditons sulfate-chloride exchange becomes electrogenic, and a positive charge on the protein now accompanies Cl^- transport. Jennings (1995) reasoned that in unmodified cells, during normal Cl^- translocation the mobile positive charge is neutralized by the negative charge on glutamate 681 which must itself traverse most of the transmembrane electric field. The negative gating charge that is consistent with DIDS-insensitive Cl^- conductance is not necessarily glutamate 681, although this amino acid would be a possible candidate if the fluxes turn out to be mediated by capnophorin by a voltage-gated mechanism.

Since capnophorin (AE1) functions mainly as an electroneutral exchanger with "ping-pong" kinetics (Gunn and Fröhlich, 1979; Jennings, 1982), it would be of considerable interest to find indications of gating properties from analysis of current-voltage curves. The red cell membrane resistance has been estimated at around $10^6\ \Omega \cdot cm^2$, corresponding to a total membrane conductance of around 25 pS/cell (Hoffman et al., 1980). Capnophorin (AE1) is the most prevalent integral glycoprotein in the red cell membrane. If this con-

ductance were uniformly distributed among the $1.2(10^6)$ band 3 monomers per cell, the "single channel conductance" would be of the order of 10^{-5} pS, making it unlikely ever to be able to observe such channel gating directly. Alternatively, one or a few DIDS-insensitive background chloride channels per cell could account for the Cl^- currents observed in this study. Preliminary observations of anion selective channels in human red blood cells have been recorded with the patch clamp technique (Schwarz et al., 1989), and also after fusing vesicles from red cell suspensions into planar lipid bilayers (Freedman and Miller, 1984). Additional biophysical studies of chloride conductance, together with structural and molecular biological studies, should potentially aid in relating the mechanisms of conductance and exchange, and in revealing the detailed mechanism of chloride transport across red cell membranes.

We thank Drs. P. Stampe, E. Moczydlowski, P. Pratap, and P. Dunham for valuable discussions, and for reading and commenting on a draft of the manuscript. We thank DeForest Brooker, Hematology Supervisor, Division of Clinical Pathology, SUNY Health Science Center at Syracuse, for use of the Technicon H-1 Hematology Analyzer and for phlebotomy services. We also thank Christopher J. Perigard, Clinical Pathology Supervisor, Bristol-Myers Squibb Company, Pharmaceutical Research Institute (Syracuse, NY) for use of the Technicon H-1 Hematology Analyzer.

We gratefully acknowledge the initial support of National Institutes of Health grant GM28839, continued support from the Department of Physiology and the Hendrick's Fund for Medical Research of SUNY Health Science Center at Syracuse, and a grant from the National Kidney Foundation of Central New York, Inc.

Original version received 27 November 1995 and accepted version received 1 November 1996.

REFERENCES

Alper, S.L. 1991. The band 3-related anion exchanger (AE) gene family. *Annu. Rev. Physiol.* 53:549–564.

Andersen, O.S. 1983*a*. Ion movement through gramicidin A channels. Single-channel measurements at very high potentials. *Biophys. J.* 41:119–133.

Andersen, O.S. 1983*b*. Ion movement through gramicidin A channels. Studies on the diffusion-controlled association step. *Biophys. J.* 41:147–165.

Bartel, D., H. Hans, and H. Passow. 1989. Identification by site-directed mutagenesis of Lys-558 as the covalent attachment site of H_2DIDS in the mouse erythroid band 3 protein. *Biochim. Biophys. Acta.* 985:355–358.

Barzilay, M., S. Ship, and Z.I. Cabantchik. 1979. Anion transport in red blood cells. I. Chemical properties of anion recognition sites as revealed by structure-activity relationships of aromatic sulfonic acids. *Membr. Biochem.* 2:227–254.

Batenjany, M.M., H. Mizukami, and J.M. Salhany. 1993. Near-UV circular dichroism of band 3. Evidence for intradomain conformational changes and interdomain interactions. *Biochemistry.* 32: 663–668.

Bennekou, P. 1984. K^+-Valinomycin and chloride conductance of the human red cell membrane. Influence of the membrane protonophore carbonylcyanide *m*-chlorophenylhydrazone. *Biochim. Biophys. Acta.* 776:1–9.

Bennekou, P. 1988. Protonophore anion permeability of the human red cell membrane determined in the presence of valinomycin. *J. Membr. Biol.* 102:225–234.

Bennekou, P., and P. Christophersen. 1986. Flux ratio of valinomycin-mediated K^+ fluxes across the human red cell membrane in the presence of the protonophore CCCP. *J. Membr. Biol.* 93:221–227.

Bennekou, P., and P. Stampe. 1988. The effect of ATP, intracellular calcium and the anion exchange inhibitor DIDS on conductive anion fluxes across the human red cell membrane. *Biochim. Biophys. Acta.* 942:179–185.

Bezanilla, F. 1994. Voltage-dependent gating of ionic channels. *Annu. Rev. Biophys. Biomol. Struct.* 23:819–846.

Bifano, E.M., T.S. Novak, and J.C. Freedman. 1984. The relationship between the shape and the membrane potential of human red blood cells. *J. Membr. Biol.* 82:1–13.

Cabantchik, Z.I., and A. Rothstein. 1972. The nature of the membrane sites controlling anion permeability of human red blood cells as determined by studies with disulfonic stilbene derivatives. *J. Membr. Biol.* 10:311–330.

Chesnoy-Marchais, D. 1983. Characterization of a chloride conductance activated by hyperpolarization in *Aplysia* neurones. *J. Physiol. (Lond.).* 342:277–308.

Deuticke, B., E. Beyer, and B. Forst. 1982. Discrimination of three parallel pathways of lactate transport in the human erythrocyte membrane by inhibitors and kinetic properties. *Biochim. Biophys. Acta.* 684:96–110.

Falke, J.J., and S.I. Chan. 1986*a*. Molecular mechanism of band 3 inhibitors. I. Transport site inhibitors. *Biochemistry.* 25:7888–7894.

Falke, J.J., and S.I. Chan. 1986*b*. Molecular mechanism of band 3 inhibitors. 2. Channel blockers. *Biochemistry.* 25:7895–7898.

Freedman, J.C., E.M. Bifano, L.M. Crespo, P.R. Pratap, R. Wallenga, R.E. Bailey, S. Zuk, and T.S. Novak. 1988. Membrane potential and the cytotoxic Ca cascade of human red blood cells. *In* Cell Physiology of Blood. R.B. Gunn and J.C. Parker, editors. Society of General Physiologists Series, The Rockefeller University Press, New York, NY. 218–231.

Freedman, J.C., and J.F. Hoffman. 1979*a*. Ionic and osmotic equilibria of human red blood cells treated with nystatin. *J. Gen. Physiol.* 74:157–185.

Freedman, J.C., and J.F. Hoffman. 1979*b*. The relation between dicarbo-cyanine dye fluorescence and the membrane potential of human red blood cells set at varying Donnan equilibria. *J. Gen. Physiol.* 174:187–212.

Freedman, J.C., and C. Miller. 1984. Membrane vesicles from human red blood cells in planar lipid bilayers. *Ann. NY Acad. Sci.* 435:541–544.

Freedman, J.C., and T.S. Novak. 1983. Membrane potentials associated with Ca-induced K conductance in human red blood cells. Studies with a fluorescent oxonol dye, WW781. *J. Membr. Biol.* 72: 59–74.

Freedman, J.C., and T.S. Novak. 1984. K and Cl conductance of valinomycin treated human red blood cells, as determined with the fluorescent potentiometric indicator WW781. *J. Gen. Physiol.*

184:18*a*. (Abstr.)

Freedman, J.C., and T.S. Novak. 1987. Chloride conductance of human red blood cells at varied E_K. *Biophys. J.* 51:565*a*. (Abstr.)

Freedman, J.C., and T.S. Novak. 1989. Optical measurements of membrane potential in cells, organelles, and vesicles. *Methods Enzymol.* 172:102–122.

Freedman, J.C., and T.S. Novak. 1996. Equivalent gating charge of DIDS-insensitive chloride conductance in human red blood cells treated with valinomycin or gramicidin. *Biophys. J.* 70:A241. (Abstr.)

Freedman, J.C., T.S. Novak, J.D. Bisognano, and P.R. Pratap. 1994. Voltage dependence of DIDS-insensitive chloride conductance in human red blood cells treated with valinomycin or gramicidin. *J. Gen. Physiol.* 104:961–983.

Fröhlich, O., C. Leibson, and R.B. Gunn. 1983. Chloride net efflux from intact erythrocytes under slippage conditions. *J. Gen. Physiol.* 81:127–152.

Funder, J., and J.O. Wieth. 1976. Chloride transport in human erythrocytes and ghosts: a quantitative comparison. *J. Physiol. (Lond.).* 262:679–698.

Garcia, A.M., and H.F. Lodish. 1989. Lysine 539 of human band 3 is not essential for ion transport or inhibition by stilbene disulfonates. *J. Biol. Chem.* 264:19607–19613.

Gasbjerg, P.K., J. Funder, and J. Brahm. 1993. Kinetics of residual chloride transport in human red blood cells after maximum covalent 4,4′-diisothiocyanostilbene-2,2′-disulfonic acid binding. *J. Gen. Physiol.* 101:715–732.

Goldman, D.E. 1943. Potential, impedance and rectification in membranes. *J. Gen. Physiol.* 27:37–60.

Gunn, R.B. 1978. Considerations of the titratable carrier model for sulfate transport in human red blood cells. *In* Membrane Transport Processes. Vol. 1. J.F. Hoffman, editor. Raven Press, New York, NY. 61–77.

Gunn, R.B., and O. Fröhlich. 1979. Asymmetry in the mechanism for anion exchange in human red blood cell membranes. Evidence for reciprocating sites that react with one transported anion at a time. *J. Gen. Physiol.* 74:351–374.

Hall, J.E., C.A. Mead, and G. Szabo. 1973. A barrier model for current flow in lipid bilayer membranes. *J. Membr. Biol.* 11:75–97.

Hanrahan, J.W., W.P. Alles, and S.A. Lewis. 1985. Single anion-selective channels in basolateral membrane of a mammalian tight epithelium. *Proc. Natl. Acad. Sci. USA.* 82:7791–7795.

Hille, B. 1992. Ionic channels of excitable membranes. 2nd edition. Sinauer Associates, Sunderland, MA. 54–57.

Hladky, S.B., and T.J. Rink. 1976. Potential difference and the distribution of ions across the human red blood cell membrane: a study of the mechanism by which the fluorescent cation, diS-$C_3(5)$ reports membrane potential. *J. Physiol (Lond.).* 263:287–319.

Hodgkin, A.L., and A.F. Huxley. 1952. A quantitative description of membrane current and its application to conduction and excitation in nerve. *J. Physiol. (Lond.).* 117:500–544.

Hodgkin, A.L., and B. Katz. 1949. The effect of Na ions on the electrical activity of the giant axon of the squid. *J. Physiol. (Lond.).* 108:37–77.

Hoffman, J.F., and P.C. Laris. 1974. Determination of membrane potential in human and amphiuma red blood cells by means of a fluorescent probe. *J. Physiol. (Lond.).* 239:519–552.

Hoffman, J.F., J.H. Kaplan, T.J. Callahan, and J.C. Freedman. 1980. Electrical resistance of the red cell membrane and the relation between net anion transport and the anion exchange mechanism. *Ann. NY Acad. Sci.* 341:357–360.

Hunter, M.J. 1971. A quantitative estimate of the non-exchange-restricted chloride permeability of the human red cell. *J. Physiol. (Lond.).* 218:49–50P. (Abstr.)

Hunter, M.J. 1977. Human erythrocyte anion permeabilities measured under conditions of net charge transfer. *J. Physiol. (Lond.).* 268:35–49.

Jack, J.J.B., D. Noble, and R.W. Tsien. 1983. Nonlinear properties of excitable membranes. *In* Electric Current Flow in Excitable Cells. Oxford University Press, Oxford. pp. 225–234.

Jacobs, M.H., and D.R. Stewart. 1942. The role of carbonic anhydrase in certain ionic exchanges involving the erythrocyte. *J. Gen. Physiol.* 25:539–552.

Janas, T., P.J. Bjerrum, J. Brahm, and J.O. Wieth. 1989. Kinetics of reversible DIDS inhibition of chloride self exchange in human erythrocytes. *Am. J. Physiol.* 257:C601–C606.

Jennings, M.L. 1976. Proton fluxes associated with erythrocyte membrane anion exchange. *J. Membr. Biol.* 28:187–205.

Jennings, M.L. 1982. Stoichiometry of a half-turnover of band 3, the chloride transport protein of human erythrocytes. *J. Gen. Physiol.* 79:169–185.

Jennings, M.L. 1989. Structure and function of the red blood cell anion transport protein. *Annu. Rev. Biophys. Biophys. Chem.* 18: 397–430.

Jennings, M.L. 1992. Inorganic anion transport. *In* The Structure of Biological Membranes. P. Yeagle, editor. CRC Press, Boca Raton, FL. 781–832.

Jennings, M.L. 1995. Rapid electrogenic sulfate-chloride exchange mediated by chemically modified band 3 in human erythrocytes. *J. Gen. Physiol.* 105:21–47.

Jennings, M.L., R.K. Schulz, and M. Allen. 1990. Effects of membrane potential on electrically silent transport. Potential-independent translocation and asymmetric potential-dependent substrate binding to the red blood cell anion exchange protein. *J. Gen. Physiol.* 96:991–1012.

Jennings, M.L., and J.S. Smith. 1992. Anion-proton cotransport through the human red blood cell band 3 protein. Role of glutamate 681. *J. Biol. Chem.* 267:13964–13971.

Kang, D., K. Okubo, N. Hamasaki, N. Kuroda, and H. Shiraki. 1992. A structural study of the membrane domain of band 3 by tryptic digestion. Conformational change of band 3 in situ induced by alkali treatment. *J. Biol. Chem.* 267:19211–19217.

Kaplan, J.H., M. Pring, and H. Passow. 1983. Band-3 protein mediated anion conductance of the red cell membrane. Slippage vs ionic diffusion. *FEBS Lett.* 156:175–179.

Klocke, R.A. 1988. Velocity of CO_2 exchange in blood. *Annu. Rev. Physiol.* 50:625–637.

Knauf, P.A. 1979. Erythrocyte anion exchange and the band 3 protein: transport kinetics and molecular structure. *Curr. Top. Membr. Transp.* 12:249–363.

Knauf, P.A., G.F. Fuhrmann, S. Rothstein, and A. Rothstein. 1977. The relationship between anion exchange and net anion flow across the human red blood cell membrane. *J. Gen. Physiol.* 69: 363–386.

Knauf, P.A., F.-Y. Law, and P.J. Marchant. 1983. Relationship of net chloride flow across the human erythrocyte membrane to the anion exchange mechanism. *J. Gen. Physiol.* 81:95–126.

Kopito, R.R., and H.F. Lodish. 1985. Primary structure and transmembrane orientation of the murine anion exchange protein. *Nature (Lond.).* 316:234–238.

Lassen, U.V. 1972. Membrane potential and membrane resistance of red cells. *In* Oxygen Affinity of Hemoglobin and Red Cell Acid Base Status. M. Rorth and P. Astrup, editors. Academic Press, New York, NY. 291–304.

Läuger, P. 1973. Ion transport through pores: a rate-theory analysis. *Biochim. Biophys. Acta.* 311:423–441.

Läuger, P., and G. Stark. 1970. Kinetics of carrier-mediated ion transport across lipid bilayer membranes. *Biochim. Biophys. Acta.* 211:458–466.

Lux, S. E., K. M. John, R. Kopito, and H. F. Lodish. 1989. Cloning

and characterization of band 3, the human erythrocyte anion exchange protein (AE1). *Proc. Natl. Acad. Sci. USA.* 86:9089–9093.

Macey, R. I., J. S. Adorante, and F. W. Orme. 1978. Erythrocyte membrane potentials determined by hydrogen ion distribution. *Biochim. Biophys. Acta.* 512:284–295.

Milanick, M. A., and R. B. Gunn. 1984. Proton-sulfate cotransport: external proton activation of sulfate influx into human red blood cells. *Am. J. Physiol.* 247:C247–C259.

Miller, C., and M. M. White. 1984. Dimeric structure of single chloride channels from *Torpedo* electroplax. *Proc. Natl. Acad. Sci. USA.* 81:2772–2775.

Neumke, B., and P. Läuger. 1969. Nonlinear electrical effects in lipid bilayer membranes. II. Integration of the generalized Nernst-Planck equations. *Biophys. J.* 9:1160–1170.

Nowak, L., P. Ascher, and Y. Berwald-Netter. 1987. Ionic channels in mouse astrocytes in culture. *J. Neurosci.* 7:101–109.

Passow, H. 1986. Molecular aspects of band 3 protein-mediated anion transport across the red blood cell membrane. *Rev. Physiol. Biochem. Pharmacol.* 103:61–203.

Passow, H., P.G. Wood, S. Lepke, H. Müller, and M. Sovak. 1992. Exploration of the functional significance of the stilbene disulfonate binding site in mouse band 3 by site-directed mutagenesis. *Biophys. J.* 62:98–100.

Pusch, M., and T.J. Jentsch. 1994. Molecular physiology of voltage-gated chloride channels. *Physiol. Rev.* 74:813–827.

Raftos, J.E., R.M. Bookchin, and V.L. Lew. 1996. Distribution of chloride permeabilities in normal human red cells. *J. Physiol. (Lond.).* 491:773–777.

Rao, A., P. Martin, R.A.F. Reithmeier, and L.C. Cantley. 1979. Location of the stilbenedisulfonate binding site of the human erythrocyte anion-exchange system by resonance energy transfer. *Biochemistry.* 18:4505–4516.

Reithmeier, R.A.F. 1993. The erythrocyte anion transporter (band 3). *Curr. Opin. Struct. Biol.* 3:515–523.

Sansom, S.C., B.-Q. La, and S.L. Carosi. 1990. Double-barreled chloride channels of collecting duct basolateral membrane. *Am. J. Physiol.* 259:F46–F52.

Schnell, K.F., S. Gerhardt, and A. Schöppe-Fredenburg. 1977. Kinetic characteristics of the sulfate self-exchange in human red blood cells and red blood cell ghosts. *J. Membr. Biol.* 30:319–350.

Schwarz, W., R. Grygorczyk, and D. Hof. 1989. Recording single-channel currents from human red cells. *Methods Enzymol.* 173: 112–121.

Silver, B.L. 1985. The rate theory of transport. *In* The Physical Chemistry of Membranes. Allen and Unwin, Boston, MA. Ch. 13 277–290.

Stark, G., and R. Benz. 1971. The transport of potassium through lipid bilayer membranes by the neutral carriers valinomycin and monactin. Experimental studies to a previously proposed model. *J. Membr. Biol.* 5:133–153.

Tanner, M.J.A., P.G. Martin, and S. High. 1988. The complete amino acid sequence of the human erythrocyte membrane anion transport protein deduced from the cDNA sequence. *Biochem. J.* 256:703–712.

Thiemann, A., S. Gründer, M. Pusch, and T.J. Jentsch. 1992. A chloride channel widely expressed in epithelial and non-epithelial cells. *Nature (Lond.).* 356:57–60.

Wang, D.N., W. Kühlbrandt, V.E. Sarabia, and R.A.F. Reithmeier. 1993. Two-dimensional structure of the membrane domain of human Band 3, the anion transport protein of the erythrocyte membrane. *EMBO (Eur. Mol. Biol. Organ.) J.* 12:2233–2239.

Wang, D.N., V.E. Sarabia, R.A.F. Reithmeier, and W. Kühlbrandt. 1994. Three-dimensional map of the dimeric membrane domain of the human erythrocyte anion exchanger, Band 3. *EMBO (Eur. Mol. Biol. Organ.) J.* 13:3230–3235.

White, M.M., and C. Miller. 1979. A voltage-gated anion channel from the electric organ of *Torpedo californica*. *J. Biol. Chem.* 254: 10161–10166.

Wieth, J.O., and P.J. Bjerrum. 1982. Titration of transport and modifier sites in the red cell anion transport system. *J. Gen. Physiol.* 79:253–282.

Wieth, J.O., P.J. Bjerrum, and C.L. Borders, Jr. 1982. Irreversible inactivation of red cell chloride exchange with phenylglyoxal, an arginine-specific reagent. *J. Gen. Physiol.* 79:283–312.